

## Contact formation in the silver/aluminum thick film firing process – a phenomenological approach

Stefanie Riegel, Florian Mutter, Giso Hahn, Barbara Terheiden

University of Konstanz, Department of Physics, Jacob-Burckhardt-Str. 29, 78457 Konstanz, Germany

Email: Stefanie.Riegel@uni-konstanz.de, Phone: +49 7531 88 2074, Fax: +49 7531 88 3895

**ABSTRACT:** In this paper the silver/aluminum thick film process is investigated. Aim of the work is a better understanding of the contact formation and the function aluminum fulfils. Depending on the local composition of the paste, that is the ratio of aluminum, silver and lead, different contact structures are found. These observations lead to a model explaining the contact formation for the silver/aluminum thick film process based on the model of the silver thick film process [2].

**Keywords:** boron BSF, metallization, screen print

### 1 INTRODUCTION

In the silicon based photovoltaics there are several options to obtain a p-type doping of the silicon. Commonly aluminum paste is screen printed and cofired to realize a back surface field on p-type material or an emitter on n-type substrate. Another possibility to provide a p-doped region is the diffusion of boron into the substrate. The boron diffusion has the advantage to reach a higher doping concentration leading to better surface passivation compared to screen printed aluminum.

Using silver aluminum pastes for B-BSF contacting the main problems during contact formation are high contact resistances ( $R_C$ ) due to the depletion zone and an increased saturation current ( $J_{0e}$ ) [1]. It is assumed [3], that the contact formation to  $p^+$ -Si layers is dominated by silver crystallites as shown for  $n^+$  layers [2]. Adding aluminum to the silver thick film paste reduces the specific contact resistance and enhances the amount of crystallites contacting the wafer [1, 3]. Nevertheless, the process of crystal growth from silver/aluminum paste to  $p^+$  silicon is not known up to now.

In this paper we examine the contact formation in the silver/aluminum thick film process using SEM and EDX analysis.

### 2 EXPERIMENTAL

For sample preparation  $\langle 100 \rangle$  oriented Cz p-type wafers of  $\sim 2 \Omega \text{cm}$  resistivity are used (surface doping  $\sim 1 \text{E}16 \text{cm}^{-3}$ ). The saw damage is removed in hot NaOH (80°C). The  $p^+$  region is formed via  $\text{BBr}_3$  diffusion resulting in a sheet resistivity of  $60 \Omega/\square$  (peak doping is  $1 \text{E}219 \text{cm}^{-3}$ , surface doping is  $9 \text{E}18 \text{cm}^{-3}$ ). The doping profile is shown in Figure 1. No antireflection coating is used. Contact formation is done via screen printing a finger grid and firing at different peak temperatures. Two firing processes are applied. We use the standard firing process with varying peak temperatures (800-880°C). Additionally samples are fired at lower temperatures to learn more about the thermochemistry of the contact formation. Therefore the samples are fired for  $\sim 2 \text{ s}$  at 290, 575, 625 and 710°C wafer temperature. These temperatures are below the eutectic points of lead and silver (304°C), lead and aluminum (327°C) and above the ternary point of the silver aluminum lead system and the silver aluminum silicon system ( $\sim 550^\circ\text{C}$ ) and the monotectic point of the aluminum lead system (659°C) [4-7]. Commercially available silver and silver/aluminum thick film pastes are used. For each paste three samples

per peak temperature are processed. On the first sample the metal paste is retained, on the second sample the metal paste is removed in HF (5%) and on the third sample the metal paste is removed with  $\text{NH}_4\text{OH}:\text{H}_2\text{O}_2$  (1:1) up to the glass layer at the wafer paste interface.

The specific contact resistance  $R_C$  is obtained using the transfer length method (TLM). The contact areas are investigated by a scanning electron microscope (SEM) and energy-dispersive X-ray spectroscopy (EDX) surface and interface analysis.

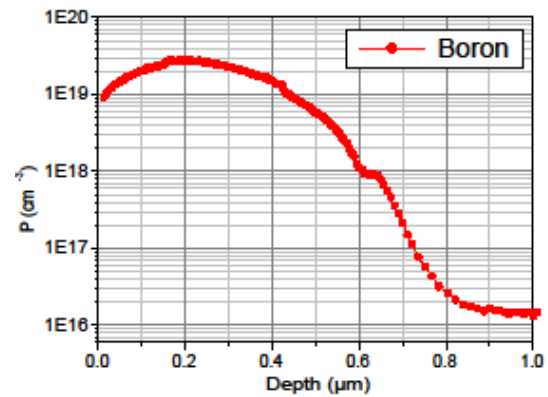


**Figure 1:** Profile after boron diffusion. Peak doping is  $2 \text{E}19 \text{cm}^{-3}$ . Surface doping is  $9 \text{E}18 \text{cm}^{-3}$ .

### 3 RESULTS

#### 3.1 Silver thick film paste on $p^+$ silicon

Contacting highly p-doped silicon with pure silver thick film paste results in specific contact resistances  $R_{C, Ag, p^+} = 58\text{-}128 \text{ m}\Omega\text{cm}^2$ . Other authors measured similar values for  $R_{C, Ag, p^+}$  of screen printed silver thick film paste on highly p-doped silicon before [1, 3]. After removing of the silver thick film paste in diluted HF ( $\sim 5\%$ ) very small silver crystallites and inverted pyramids are observed ( $< 0.5\text{-}1 \mu\text{m}$  in diameter). The number and size of crystallites and inverted pyramids does not increase with increasing firing temperature. The pyramids occur in groups of 5-20 pyramids preferably along the  $\langle 111 \rangle$  edges caused by damage etching in hot NaOH. Enhanced formation of silver pyramids along  $\langle 111 \rangle$  planes was observed for silver thick film contact formation to highly n-doped silicon as well [2].

#### 3.2 Silver/aluminum thick film paste on $p^+$ silicon

Contacting highly p doped silicon with silver aluminum thick film paste the specific contact resistance is reduced to  $R_{C, Ag/Al, p^+} = 0.7\text{-}7 \text{ m}\Omega\text{cm}^2$  at  $T_{\text{peak}} = 840$  or

860°C depending on the paste. Other authors reported  $R_{C, Ag/Al, p+}=3-4 \text{ m}\Omega\text{cm}^2$  (peak doping is  $1\text{E}20 \text{ cm}^{-3}$ ) [1].

The contact interfaces of the samples fired at different peak temperatures vary in number, size and shape of the contact spots. The size of the contact spots varies from  $\sim 0.5-4 \mu\text{m}$  ( $T_{\text{peak}}=800^\circ\text{C}$ ) to  $>11 \mu\text{m}$  ( $T_{\text{peak}}=880^\circ\text{C}$ ). After firing at  $800^\circ\text{C}$  the contact spots are broadly distributed over the metalized area (distance 5-50  $\mu\text{m}$ ). With increasing peak temperature ( $T_{\text{peak}}>820^\circ\text{C}$ ) the number of contact spots increases and they cluster in groups of up to 50 spots. For  $T_{\text{peak}}=840^\circ\text{C}$  and above the contact spots within a cluster compound to larger areas ( $>25 \mu\text{m}$ ).

At  $T_{\text{peak}}=800-820^\circ\text{C}$  most of the contact spots have a rounded shape. The rounded spots are surrounded by aluminum doped rectangles (see Fig. 2) and filled with silver and aluminum (Fig. 2 point 3, 4; Fig. 3, 4). For  $T_{\text{peak}}=820-880^\circ\text{C}$  the contact spots are more rectangular in shape. At the silicon-paste interface within the contact spots aluminum rich areas are detected (see Fig. 3 upper part, Fig. 4 point 1). The filling of the contact spots either consists of a mixture of silver, aluminum and lead (Fig. 3, 4) or it contains lamellas and crystallites (Fig. 5, 6). For the contact spot shown in Figure 5 it is confirmed via EDX analysis that the crystallites consist of silver. The lamellas are mainly composed of aluminum. The space between the lamellas is filled with silver. Due to the limited spatial resolution of the EDX measurement an element analysis is not possible for the contact spot shown in Figure 6. The resolution of an EDX system is restricted by the electron beam. For the system used in this work the resolution is restricted to  $\sim 0.5-1 \mu\text{m}$ .

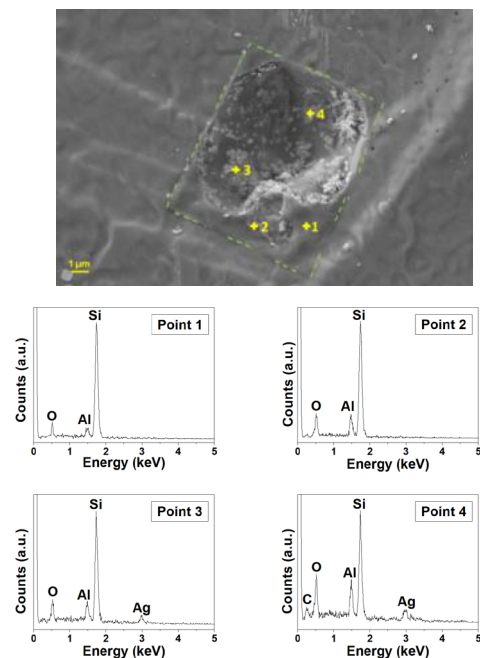


**Figure 2:** Silver/aluminum contact after etching in HF (5%).  $T_{\text{peak}}=820^\circ\text{C}$ . The contact is  $7.7 \mu\text{m}$  wide and  $10.2 \mu\text{m}$  long. The contact area is surrounded by a rectangle consisting of aluminum and oxygen (EDX spectra of point 1 and 2). Within the contact at points 3 and 4 silver is detected as well.

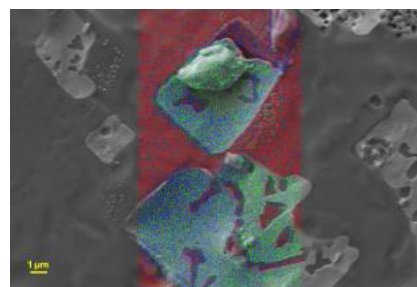


**Figure 3:** SEM micrograph and EDX scan of the contact area after etching in HF (5%).  $T_{\text{peak}}=800^\circ\text{C}$ . Red: silicon, green: silver, Blue: aluminum. Most part of the contact area is filled with silver and aluminum. In the lower right part of the scan area only silver is detected. A part of the paste filling the upper contact is lifted. Therefore the interface between silver/aluminum thick film paste and silicon wafer is visible. At the silicon-paste interface aluminum is detected.

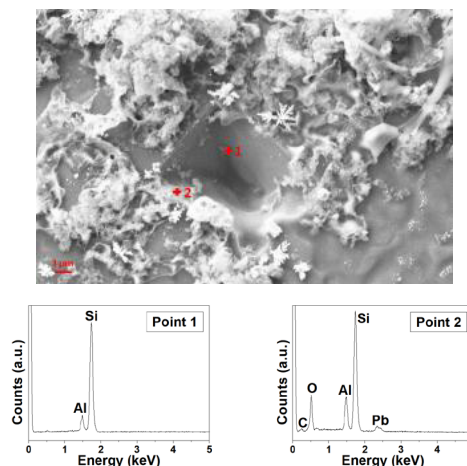


**Figure 4:** Silver/aluminum paste after etching in  $\text{NH}_4\text{OH}:\text{H}_2\text{O}_2$  (1:1).  $T_{\text{peak}}=820^\circ\text{C}$ . Aluminum silver lead silicon structures remain after etch back. At the wall of the pyramid (point 1) only aluminum and silicon are detected. At point 2 at the edge to the wafer surface carbon, oxygen and lead are found as well.

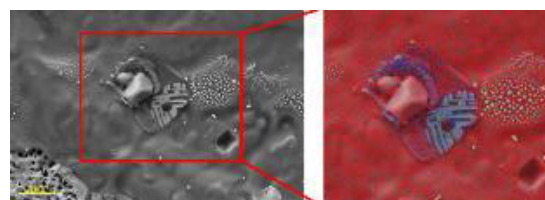


**Figure 5:** Silver/aluminum contact after etching in HF (5%).  $T_{\text{peak}}=880^\circ\text{C}$ . The area marked with the red box was measured with an EDX scan. Red: silicon, green: silver, blue: aluminum. One can see that the pellets in the right part of the contact consist of silver while the walls or lamellas in the middle of the red box consist of aluminum.

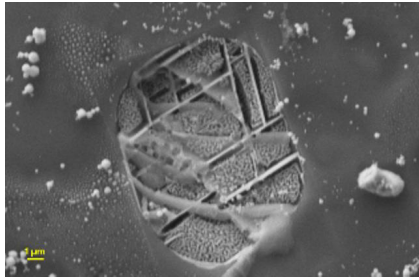


**Figure 6:** Silver/aluminum contact after etch back in HF (5%).  $T_{\text{peak}}=800^{\circ}\text{C}$ . Size is  $3.2\times 2.2\ \mu\text{m}$ . The substructures are smaller than 600 nm. Therefore they are too small to be dissolved with our EDX system. The system is limited by the diameter of the electron beam.

To learn more about the synthesis of the contact spots samples are fired at lower peak temperatures (290, 575, 625 and  $710^{\circ}\text{C}$ , for details see section 2). Though we do not observe melting of the lead oxide after firing at  $290^{\circ}\text{C}$ , single contact points ( $<1\ \mu\text{m}$ ) are found already. After etching in diluted HF (5%) we find silver pellets grown into the wafer surfaces. After firing at  $575^{\circ}\text{C}$  most of the lead oxide is molten. Only few nuggets of not molten lead remain. Rounded contact points (1-2  $\mu\text{m}$  in diameter) containing silver and a very small amount of aluminum are found. The aluminum concentration detected on these samples is slightly above the detection limit of our EDX system. Rectangular shapes are detected on the wafer surface. EDX analysis revealed that these structures consist of aluminum. The specific contact resistance of these samples  $R_{C, \text{Ag/Al, p}^+}$  varies between 3 and  $60\ \text{m}\Omega\text{cm}^2$ . For the samples fired at  $625^{\circ}\text{C}$  it is reduced to  $R_{C, \text{Ag/Al, p}^+}=5-8\ \text{m}\Omega\text{cm}^2$ . The number of contact points increases. The contact spots are partly surrounded by rectangular aluminum containing forms. The contact spots are inverted pyramids or have a rounded shape. After etching in diluted HF (5%) we find many of them filled with lamellas and/or pellets. The lamellas and pellets are too small for EDX analysis. After firing at  $710^{\circ}\text{C}$  the number and size of contact spots increases further (0.5-3  $\mu\text{m}$  in diameter). It remains too small for EDX analysis of the fillings. The specific contact resistance  $R_{C, \text{Ag/Al, p}^+}$  lies in the same range as for the samples fired at  $625^{\circ}\text{C}$ .

#### 4 DISCUSSION

Based on the observations above an extension of the model from G. Schubert for the growth mechanism of silver crystallites in a silver thick film firing process [3] for the silver/aluminum thick film process is proposed.

As during the silver thick film firing process, liquid lead forms during firing due to the etching mechanism of lead borosilicate glass with silicon. Once the liquid lead comes into contact with the silver and aluminum particles, the particles melt and form a liquid silver/aluminum/lead phase (Fig. 7b). Additionally silicon from the wafer surface dissolves into the liquid (Fig. 7c). Depending on the surface conditions, in particular the thickness of the native oxide, and the local composition of the thick film paste silver/aluminum/lead spikes grow into the wafer (Fig. 7d). The spiking starts at  $\sim 290^{\circ}\text{C}$  already.

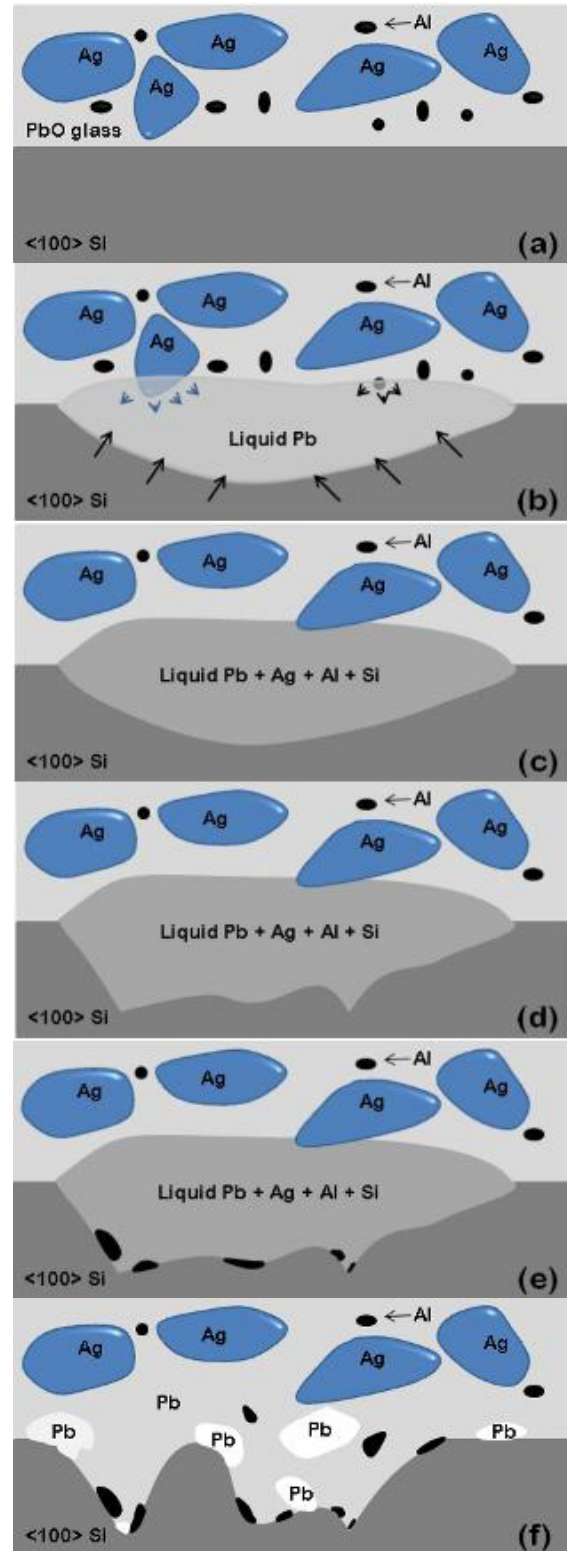


**Figure 7:** Model for the contact formation in the silver/aluminum thick film firing process. (a) Cross section of silver/aluminum thick film paste on  $\langle 100 \rangle$  oriented silicon after burn out. (b) Liquid lead has formed and reacts with the silicon wafer and aluminum and silver contained in the paste. (c) Silicon interacts with the liquidus. (d) Aluminum precipitates at the silicon liquidus interface. (e) The liquidus freezes.

In the SEM and EDX micrographs (see section 3.2, Fig. 2, 3, 4) aluminum precipitates are found at the

silicon paste interface. Looking into the phase diagrams of alloys of elements contained in the silver/aluminum thick film paste, we find the monotectic point of the aluminum/lead system at  $T=659^{\circ}\text{C}$  and the eutectic points of the lead/aluminum/silicon system and the silver/aluminum/silicon system at  $T=550^{\circ}\text{C}$ . Assuming that these points exist in the more complex system of the silver/aluminum thick film paste as well – though at lower temperatures, below  $625^{\circ}\text{C}$  – we suppose that aluminum precipitates at the silicon liquidus interface when the temperature falls below the monotectic temperature of the aluminum lead sub-system. This precipitation of aluminum leads to the aluminum doped rectangles around the contact spots observed above (Fig. 2). Due to the fact that we observe aluminum rectangles after firing at  $575^{\circ}\text{C}$  already, another possible mechanism for silver/aluminum contact formation is the promotion of contact formation by aluminum doped silicon. This means contact spots arise within the aluminum doped rectangles preferably. This formation path explains the fact that we do not detect aluminum doped rectangles on samples fired at temperatures above  $575^{\circ}\text{C}$ . At the eutectic points of the lead/aluminum/silver system and the silver/aluminum/silicon system the liquidus freezes (Fig. 7e, f). If the elements are present in the eutectic composition, the liquidus crystallizes. If the elements are not present in the eutectic composition the liquidus solidifies amorphous. Hereby regions of different element composition are formed (Fig. 7f; Fig. 3 lower part; Fig. 5, 6).

## 5 SUMMARY

The contact formation to highly p-doped silicon with silver thick film paste needs to be promoted by aluminum as other authors showed before [1, 3]. For the silver/aluminum thick film process used to contact highly p-doped silicon wafers an extension of the model for the growth mechanism of pure silver crystallites in a silver thick film firing process [3] is proposed. The contact formation between silver/aluminum thick film paste and highly p-doped silicon is greatly influenced by the amount of aluminum, silver and lead in the paste. Depending on the composition of the paste different contact formation paths are possible. Aluminum within the metal paste lowers the melting point of the paste and promotes the growth of contact spots into the wafer. Aluminum at the silicon wafer surface melts and forms aluminum doped regions on the silicon wafer. In these aluminum doped areas the growth of silver/aluminum/lead spikes is enhanced. The dependency on the composition of the paste results in a locally varying shape of the contact spots. If the local composition of the paste is dominated by silver or aluminum, the contact formation works in the same way as for pure silver or aluminum paste. At these points we find silver pellets and aluminum lamellas in the SEM micrograph.

## 6 ACKNOWLEDGEMENTS

The authors would like to thank L. Rothengaß for the support during cell processing, S. Öner for some of the SEM micrographs and A. Zuschlag for introduction to SEM and EDX.

The financial support from the BMU projects FKZ 0325079 and 0325168 is gratefully acknowledged. The content of this publication is the responsibility of the authors.

## 7 REFERENCES

- [1] R. Lago et al., *Screen printing metallization of boron emitters*, Progress in Photovoltaics: Research and Applications, 2010, **18**, 20-27.
- [2] G. Schubert, *Thick film metallization of crystalline silicon solar cells: mechanisms, models and applications*, PhD thesis, University of Konstanz, 2006.
- [3] H. Kerp et al., *Development of screenprintable contacts for  $p^+$  emitters in bifacial solar cells*, Proc. 21<sup>st</sup> EU PVSEC Dresden, 2006, 892-894.
- [4] R. W. Olesinski et al., *The Pb-Si (Lead-Silicon) system*, Bulletin of Alloy Phase Diagrams, 1987, **8**(4), 326-334.
- [5] A. J. McAlister, *The Al-Pb (Aluminum-Lead) System*, Bulletin of Alloy Phase Diagrams, 1984, **5**(1), 69-73.
- [6] U. Kattner, *Silver-Aluminum-Silicon*, Ternary Alloys, 1998, **1**, 71-73.
- [7] S. Jönsson, *Silver-Aluminum-Lead*, Ternary Alloys, 1998, **1**, 59-61.